Desalination and Water Treatment
www.deswater.com

doi: 10.5004/dwt.2019.24723

170 (2019) 80–90
December

Preparation of thin film composite membranes using interfacial polymerization for treatment of industrial water containing heavy metals

Ibtissem Ounifi[a,b,*], Claudia Ursino[c], Amor Hafiane[a], Alberto Figoli[c], Ezzedine Ferjani[d]

[a]*Laboratory of Water, Membrane and Environmental Biotechnology, Centre of Research and Water Technologies, Technopark of Borj-Cedria, BP 273, 8020 Soliman, Tunisia, emails: ibtissemounifi@yahoo.com (I. Ounifi), amor.hafiane@certe.rnrt.tn (A. Hafiane)*
[b]*Faculty of Sciences of Tunis, University of Tunis - El Manar, 20 Tolede street, Tunis 2092*
[c]*Institute on Membrane Technology (ITM-CNR), Via P. Bucci 17 c, 87036 Rende (CS), Italy, emails: claudiaursino@gmail.com (C. Ursino), a.figoli@itm.cnr.it (A. Figoli)*
[d]*Higher Institute of Science and Technology of Environment of Borj-Cedria, Bp 2050 Borj-Cedria, Tunisia, email: ezz_ferj@yahoo.com*

Received 24 December 2018; Accepted 24 July 2019

ABSTRACT

Polyamide thin film composite nanofiltration (NF-TFC) membranes were prepared by interfacial polymerization (IP) method using synthetic cellulose acetate membranes as support. M-phenylenediamine (MPD) and trimesoyl chloride (TMC) were used as monomers in water and hexane solution respectively. The effect of different monomers concentrations varying from 0.1 to 0.25 wt.% and IP times from 15 to 90 s were investigated. The surface of different produced membranes were characterized using the scanning electron microscopy, atomic force microscopy, Fourier-transform infrared, contact angle (CAw) and porosity. Water permeability and salts rejection (NaCl, Na_2SO_4) were determined for testing the membranes performances. The permeation studies showed that depending on TMC concentration and IP reaction time, the water permeabilities were 23.57 and 10.44 (L m^{-2} h^{-1} bar^{-1}), respectively. Na_2SO_4 and NaCl rejections were varying from 69.23% to 92.43% and from 19% to 55.54%, respectively, when TMC concentration was between 0.1% and 0.25% (w/v). The results of cadmium solution retention indicated that these novel membranes could be successfully applied for the heavy metals removal. The maximum of cadmium rejection at 0.25% (v/w) TMC concentration is 97.76% for $CdSO_4$. This cadmium rejection depend on the nature of associated anion: $R(Cd(NO_3)_2) < R(CdCl_2) < R(CdSO_4)$.

Keywords: Polyamide; Thin film composite; Nanofiltration membrane; Interfacial polymerization; Heavy metals

1. Introduction

The membrane is defined as a selective barrier that permits the separation of molecules or ions in a liquid by a combination of sieving and diffusion mechanisms. Indeed, nowadays, membrane processes have more attention due to their several advantages: easy operation, high efficiency and no or little need for chemicals products. Among various membrane separation processes, nanofiltration (NF) is a relatively recent technology (since 1980), classed between ultrafiltration (UF) and reverse osmosis (RO). Additionally to its interesting features, the removal of organic matter and nearly all viruses with molecular weight cut off between 100 and 1,000 Da [1,2]. It has also a good selectivity for multivalent ions that removes divalent ions. So NF is often used to soften hard water.

The nanofiltration was rapidly developed for different applications such as: drinking water production [3], wastewater treatment and water recycling. It was very efficient in dyes elimination [4], textile processing effluents and removal of toxic heavy metals such as: arsenic [5], chrome [6], lead [7] and

* Corresponding author.

nickel [8]. Furthermore, several membrane separation studies are reported for removal of heavy metals particularly cadmium (Cd^{2+}). In fact, the cadmium has been characterized by the high affinity for proteins and by the bioaccumulation in organisms which causes a progressive chronic poisoning. Moreover, it is known that the cadmium causes lung cancer, affects the respiratory system, kidney, liver, renal failure, human carcinogen, weakens the bone, respiratory disease, gastrointestinal diseases, birth defects, anaemia and inhibits the calcium control in biological systems [9–11]. The World Health Organization (WHO) establishes that the maximum concentration of cadmium, tolerated in drinking water has been set 5 μ L^{-1} [12].

Generally, the most developed NF membranes comprise thin-film composite structure [2], with a selective skin on top of the porous support. Many techniques have been developed to prepare these types of membranes, including plasma initiated polymerization [13], photo-initiated polymerization [14], layer by layer [15] and interfacial polymerization (IP) [14,16]. Among the different techniques, interfacial polymerization adopted a particular interest. In fact, this technique is considered as breakthrough in the preparation of membrane, reported firstly by Cadotte in 1989 [17]. It was developed in the first time for RO membranes. The advantage of interfacial polymerization is that the reaction is self-inhibiting through passage of a limited supply of reactants and it requires shorter reaction time [18]. The skin layer produced by this technique will determine the overall solute retention, permeate flux and, in general, will control the efficiency of the membrane process. The IP usually takes place at the interface between immiscible organic phases and water. Generally, the monomers used are aliphatic or aromatic diamines e.g., piperazine (PIP) [19], m-phenylenedimine (MPD) [20], bisphenol A (BPA) [21] and acid chloride monomers e.g., trimesoyl chloride (TMC) [22,23] and terephtaloyl chloride (TPC) [24]. Depending on the monomers type used, the top surface of TFC can be a polyamide [25] (formed by reaction between amine and acyl chloride), a polyurea [26] (formed by amine and cyanogen) or a polyester [18] (prepared from alcohol/phenol and acyl chloride). Polyamide (PA) is the most popular top surface for the TFC membranes. A recent study discussed by Fan et al. [27], reported the addition of inorganic salt like calcium chloride ($CaCl_2$) dissolved in water and used as an additive in the interfacial polymerization technique. The calcium ions (Ca^{2+}) were able to have complexation with carbonyl groups, which would lead to the formation of thin polyamide film.

Based on Tsuru et al. [28] study, the application of two steps of interfacial polymerization with MPD and TMC would increase the water permeability of the membrane. Also, Abou Seman et al. [29] reported an improvement on the antifouling properties and performance of membranes modified by IP where BPA and TMBPA have been used for the membrane development. The influence of monomer concentration and reaction time in IP were investigated towards the polyester NF-TFC membranes [21,30]. Other novel monomers types such as diethylenetriamine (DETA), triethylenetetramie (TETA), tetraethenepentamine (TEPA) and piperazidine (PIB) have also been studied by Li et al., [1]. Li et al. [31] reported also a new material, namely polyhexamethylene guanidine hydrochloride (PHGH), which showed good inhibition properties of bacteria and was successfully used for nanofiltration preparation by interfacial polymerization technique to be used in dyes removal (e.g., Congo Red, Methyl Orange and including Brilliant Blue) and salts ($MgCl_2$, $MgSO_4$, Na_2SO_4 and NaCl).

In this study, we presented the preparation of polyamide thin film composite nanofiltration (NF-TFC) by interfacial polymerization using the monomers m-phenylenediamie and trimesoyl chloride. The effect of different TMC concentrations and IP reaction time were investigated. These two operating parameters play an important role in the formation of the structure of the prepared skin top layer and subsequently the membrane synthesis. The chemical and physical surface properties of the prepared nanofiltration membranes were characterized in terms of morphology, FTIR, porosity and water content (WC). Membrane performances were determined by the study of pure water permeability (PWP) and salts (Na_2SO_4 and NaCl) rejection. Finally, the thin film composite nanofiltration were tested for the removal of cadmium ($CdSO_4$, $Cd(NO_3)_2$ and $CdCl_2$).

2. Experimental setup

2.1. Materials and reagents

Cellulose acetate (CA) (MW 30.000 gr mol^{-1}), acetone, formamide, m-phenylenediamine, trimesoyl chloride, hexane, sodium salts (Na_2SO_4, NaCl) cadmium Salts ($CdSO_4$, $Cd(NO_3)_2$ and $CdCl_2$) were purchased from Sigma Aldrich (Darmstadt, Germany). The chemical structures of monomers are shown in Fig. 1.

2.2. Preparation of CA support

The porous polymeric CA supports were prepared using the phase inversion technique. The casting solution consists of CA powder 19.5% wt., dissolved in a mixture of acetone and formamide (2/1) at room temperature (25°C). The solution was stirred for 24 h until complete dissolution of the polymer and then was allowed to degas for 1 h, before casting. The solution was casted into a glass plate, and was spread with a doctor's blade to be 200 μm thick. Then, the glass plate was immersed for 1 h in a distilled water coagulation bath at 4°C. The membranes were then annealed for 10 min in distilled water bath at 60°C, for the thermal treatment [32].

2.3. Preparation of nanofiltration membranes

NF-TFC membranes were prepared by interfacial polymerization technique using synthetic CA ultrafiltration

M-phenylenediamine Trimesoyl chloride

Fig. 1. Chemical structures of monomer.

(UF) membrane as support. The membrane support was taped onto a glass plate to leave only the top surface available for reaction. The cleaned membrane was immersed in a 0.2% (w/v) of m-phenylenediamine aqueous solution for 2 min at 25°C. The pre-soaked membrane was positioned vertically out from the aqueous solution for 1 min to remove the excess of the MPD from the surface of membrane support. Then, the membrane was immerged in hexane organic solution with trimesoyl chloride, for a predetermined time for interfacial polymerization reaction. Finally, the TFC membrane was dried during 10 min for the evaporation of hexane. Then, it was stored in distilled water before characterization tests.

The series of produced membranes, the concentration of TMC and the reaction times were reported in Table 1.

The IP mechanism reaction between m-phenylenediamine and trimesoyl chloride is presented in Fig. 2.

3. Membrane characterization

3.1. Scanning electron microscopy

The morphology of cross sectional and surface of the membranes were analyzed by scanning electron microscopy (SEM) (Zeiss EVO MA 100, Assing, Italy). The membranes samples were sputter-coated with a thin gold prior to SEM observation.

Table 1
Preparation condition

Membrane name	TMC %	Reaction time (sec)
UF support	0	0
TFC-0.1-15	0.1	15
TFC-0.1-30	0.1	30
TFC-0.1-90	0.1	90
TFC-0.15-15	0.15	15
TFC-0.15-30	0.15	30
TFC-0.15-90	0.15	90
TFC-0.25-15	0.25	15

3.2. Atomic force microscopy

The surface morphology and roughness of the prepared membranes were studied using atomic force microscopy (AFM) (Bruker Multimode 8 with Nanoscope V controller, Santa Barbare, CA USA). Images were acquired in tapping mode, using silicon cantilevers (mode TAP 150, Bruker, Santa Barbare, CA USA).

3.3. Fourier-transform infrared spectroscopy

The surface chemical characterization of the ultrafiltration and thin film composite membrane was detected by Fourier-transform infrared (FTIR) spectroscopy (IR Affinit-1). The spectra FTIR of the membrane was measured in transmittance mode over a wave number range of 4,000–650 cm^{-1} at 25°C.

3.4. Contact angle

The hydrophobicity nature of the membrane was determined by an optical camera using an Attension Theta T200 blood pressure monitor. It is controlled by the "One Attension Software" software. The measurements of the contact angle (CAw) and the corresponding standard deviation were taken and the average values were then calculated.

3.5. Porosity

The porosity (ε%) was determined by gravimetric method, according to literature [33]. Porosity is defined as the ratio between the volume of voids presented in the membrane and the volume of the membrane. The dry membrane was weighted and impregnated in kerosene for 24 h. After this time, the excess of kerosene was eliminated, and the membrane was weighted for the second time.

The porosity was determined as follows (1):

$$\varepsilon(\%) = \left\{ \frac{(W_w - W_d)/\rho_i}{(W_w - W_d)/\rho_i + \frac{W_d}{\rho_p}} \right\} \quad (1)$$

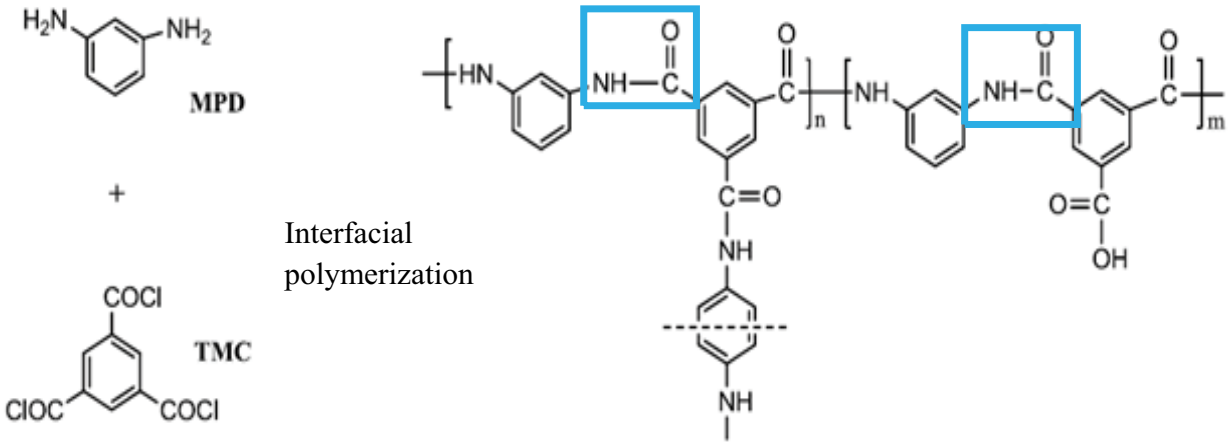

Fig. 2. Polymerization reaction between MPD and TMC.

where ε is the membrane porosity (%), W_w is the wet weight of the membrane, W_d is the dry weight of the membrane, ρ_p is the polymer density (1.28 g cm^{-3}) and ρ_k is the density of kerosene (0.82 g . cm^{-3}).

3.6. Water content

The WC of the synthesized membrane was determined according to literature as follows [34]:

$$\mathrm{WC} = \frac{m_w - m_d}{m_w} \times 100 \quad (2)$$

where m_w is the weight of the wet membrane determined after the water excess on the membrane surface's wiped, m_d is the weight of the dry membrane determined after the membrane is dried in an oven at 75°C for 24 h.

3.7. Membranes performance

TFC-NF and non-modified CA membranes were characterized by measuring the water permeability, sodium salts rejections (NaCl, Na_2SO_4) and cadmium salt rejections ($CdSO_4$, $Cd(NO_3)_2$, $CdCl_2$).

Membranes performance was determined using stainless steel cell (Millipore, Massachusetts, USA) having a total volume of 350 mL, and the effective membrane area was 38.54 cm^2. The NF set-up is represented in Fig. 3.

The permeate flux (J_v) of the membrane was measured by applying N_2 gas pressures varying from 0 to 16 bar. The permeate flux was determined using the following equation:

$$J_v = \frac{V}{A \cdot \Delta t} \quad (3)$$

where J_v is the pure water flux (L m^{-2} h^{-1}), V is the volume of permeate (L), A is the effective membrane area (m^2) and Δt is the operating time (h).

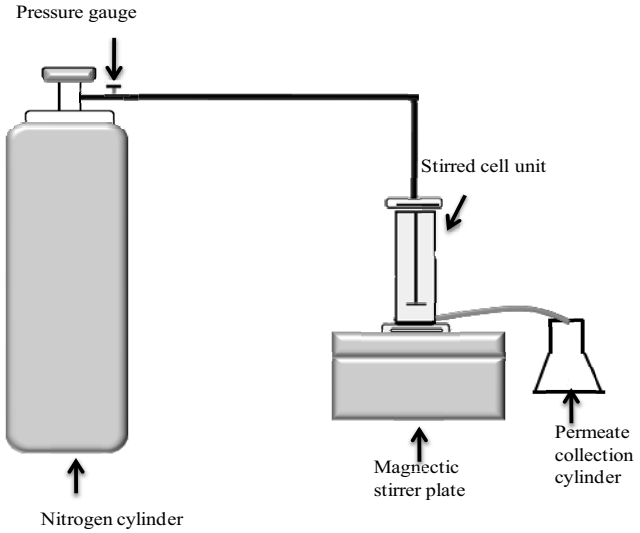

Fig. 3. Nanofiltration pilot set-up.

Sodium salts solution (Na_2SO_4, NaCl) and cadmium salts solution ($CdSO_4$, $Cd(NO_3)_2$ and $CdCl_2$) were prepared by dissolving adequate quantity into 1 L of distilled water. The feed and permeate cadmium concentrations were measured by using flam atomic absorption spectroscopy. Then, the retention rate was calculated as follows (4):

$$R(\%) = \left(1 - \frac{C_p}{C_f}\right) \times 100 \quad (4)$$

where C_f and C_p are the concentrations of feed and permeate solutions, respectively.

4. Results and discussion

4.1. Scanning electron microscopy

The morphology of both the ultrafiltration support and the thin film composite membrane were characterized by SEM. Fig. 4 shows the cross-section, top and bottom of the membranes produced by interfacial polymerization. The CA substrate presented an asymmetric structure with a microporous finger like sub layer as shown in Fig. 4. The SEM images show that the TFC nanofiltration represented a dense structure, smooth selective top layer and have a roughness structure with nodular surface structure well distributed all throughout the surface, compared to the UF membrane support common to polyamide membrane [35–37]. The cross-section images of the membranes showed that the TFC nanofiltration have presented a composite structure and the thickness of the prepared thin skin top layer which increase with the increasing MPD and/or TMC concentration in solution. The SEM images of cross-section presented in Fig. 4 have revealed the existence of the upper dense polyamide top layer which was quite thick and uniform [38].

During the IP process, the amine groups of m-phenylenediamine tend to react with acyl chloride group of trimesoyl chloride and form amide group in the chemical structure of the polyamide thin film composite membrane [39].

4.2. Atomic force microscopy

The topology of membranes surface was investigated using the AFM surface images as presented in Fig. 5. The roughness values were given in terms of root mean square roughness (RMS), roughness average (Ra) and Peak to peak (nm) in Table 2. From the AFM images, it can be observed the tiny nodules structure of polyamide on the TFC membranes surface. From 3D images, it can be seen the ridge-valley structure for TFC-NF membranes is much notable the membrane that of RMS which increased when the reaction time increased. In particular, comparing the membrane prepared using the same TMC concentration (0.1%), when the reaction time increase from 15 to 90 s, the RMS and the relative roughness average decreases, but the peak to peak value increased. This result can be explained by the fact that the reaction initially makes a smooth layer on the membrane surface. This smooth dense structure is in accordance with SEM images. For the membranes prepared using the same interfacial polymerization time (15 s) and two TMC concentrations

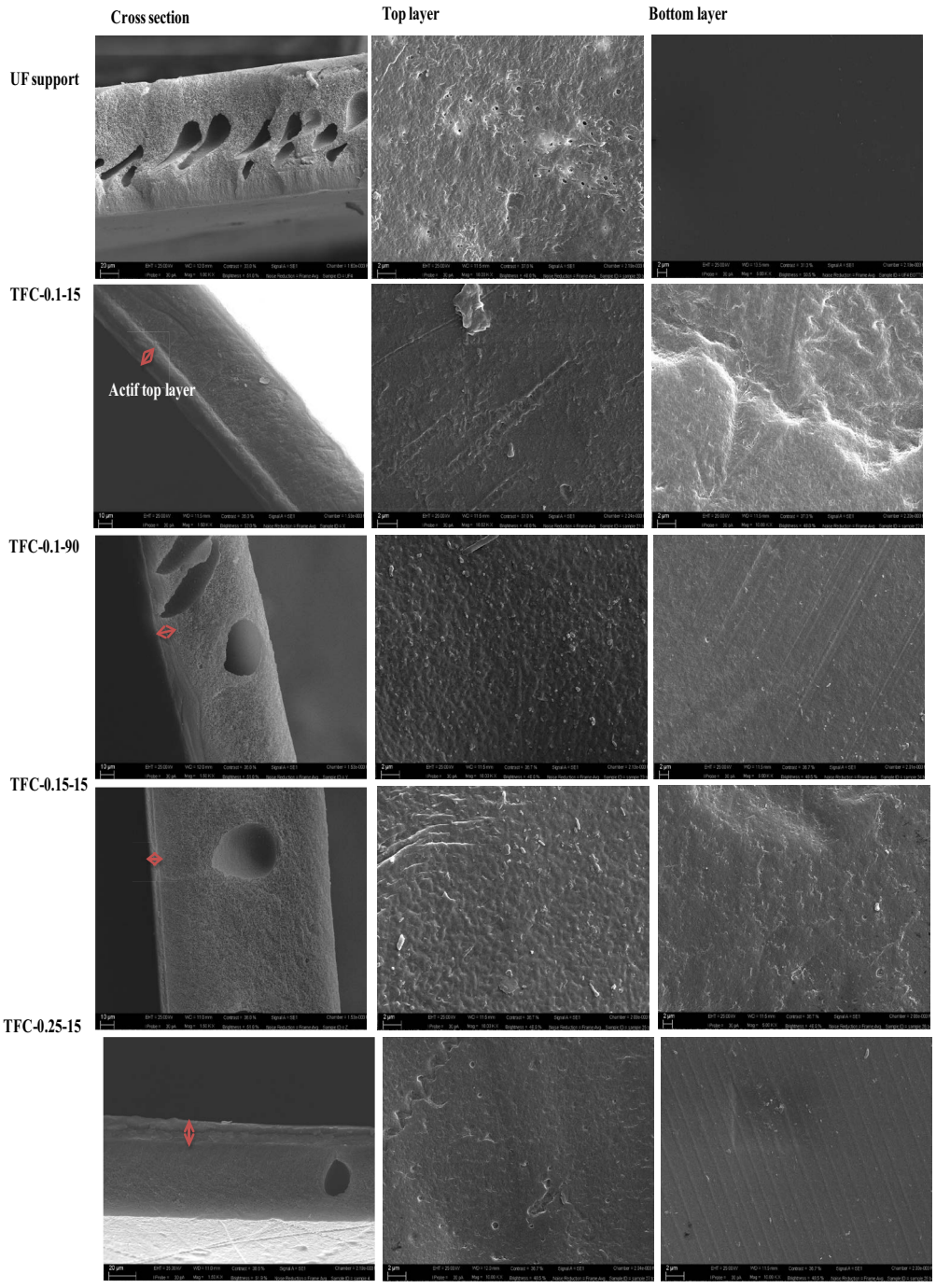

Fig. 4. SEM images of unmodified and NF-TFC polyamide membranes (Top, bottom surface and cross section images are presented).

(0.15% and 0.25%), the roughness tends to increase in correlation with monomer concentration. Both values of Ra and RMS with increasing of TMC concentration and reaction time [40–42].

4.3. Fourier-transform infrared spectroscopy

The spectra FTIR were used for characterization of the chemical surface of the membrane. The FTIR spectra of the CA support and of the TFC-NF membrane were represented in Fig. 6. For CA support, the band at 3,300–3,600 cm^{-1} was specified to OH stretching band, the bands at 1,440 and 2,930 cm^{-1} were attributed to the symmetric and asymmetric bending vibration of $–CH_2$ group, respectively. The band characteristic at 1,065 cm^{-1} was specific to C–O–C (ether linkage) from the glycosidic units. The appearance of an absorption band at 1,754 cm^{-1} is attributed to C=O vibration, followed by bands at 1,370; 1,220 and 1,060 cm^{-1}, which

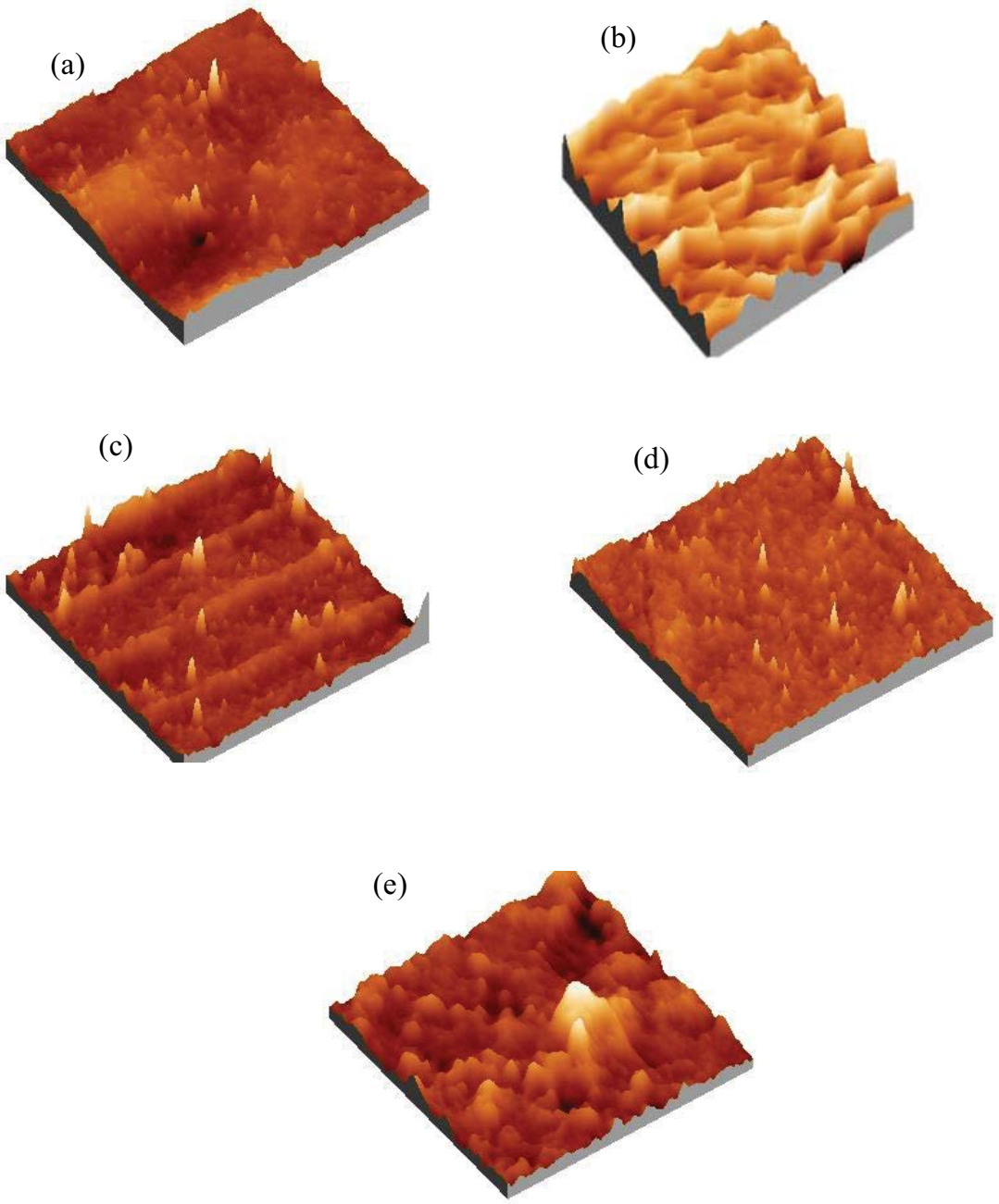

Fig. 5. AFM images of (a) unmodified and (b) TFC-0.1-15, (c) TFC-0.1-90, (d) TFC-0.15-15 and (e) TFC-0.25-15.

Table 2
RMS roughness. Roughness average and peak to peak (nm) of the membranes

Membrane name	RMS roughness (nm)	Roughness average (nm)	Peak to peak (nm)
UF support	1.69	1.53	32.27
TFC-0.1-15	3.10	12.59	5.68
TFC-0.1-90	2.68	2.26	20.34
TFC-0.15-15	3.65	2.96	25.72
TFC-0.25-15	13.24	7.30	75.20

are specified to C–O stretching of ester, carboxylic acid and ether, respectively. Compared to the CA support, tow novel bands at 1,645 and 1,545 cm^{-1} appeared on the FTIR spectra for the TFC-NF membrane comprising of a polyamide top layer [43]. This confirms that an interfacial polymerization reaction between MPD and TMC occurs and a polyamide fin top layer was formed. The tow bands at 1,645 and 1,545 cm^{-1} are specific of amide (C=O stretching) band and amide II (N–H) band of the amide groups (–CONH–). An absorption band observed at 1,720 cm^{-1} is attributed to the C=O stretching of carboxylic acids (–COOH) resulting from the hydrolysis of acyl chloride (–COCl) [37]. The bands at 2,958 and

2,850 cm^{-1} are attributed to C–H stretching that comes from methylene (–CH_2) of polyamide. The enhancement of band strength around 3,302 cm^{-1} is attributed to N–H stretching derived from the amino groups (–NH_2) of polyamide.

The TFC-NF have a specific bond of polyamide, which confirms the successful reaction between MPD and TMC and the formation of amide linkages (–CONH–) in the active thin top layer, regardless which monomer was deposited on the CA support first.

4.4. Contact angle

The hydrophilicity nature of the membranes surface was determined with CAw measurements. Fig. 7 presents the CAw of the TFC-NF membranes prepared by IP with different TMC concentrations and different reaction times. As shown in Fig. 7, it can be noticed that CAw decreased progressively from 70.32% to 39.15% when the time reaction increased from 15 to 90 s and TMC concentration increased from 0% to 0.25% (w/v). This result can be explained by the rich surface on carboxylic acid, confirmed by FTIR. In the other hand, the decrease of the contact angel can be related to the increase of the surface roughness as revealed in AFM images.

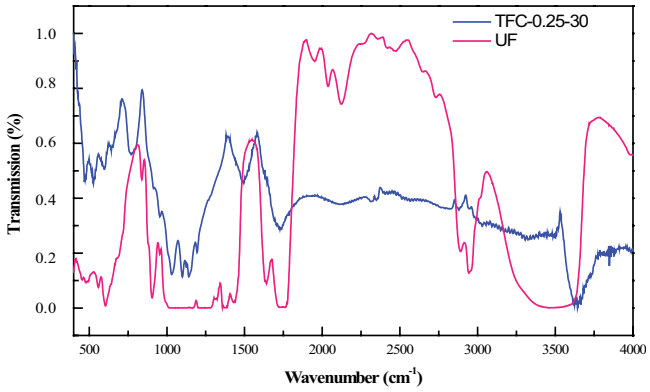

Fig. 6. FTIR spectra of (a) CA substrate and (b) composite membrane (MPD/TMC).

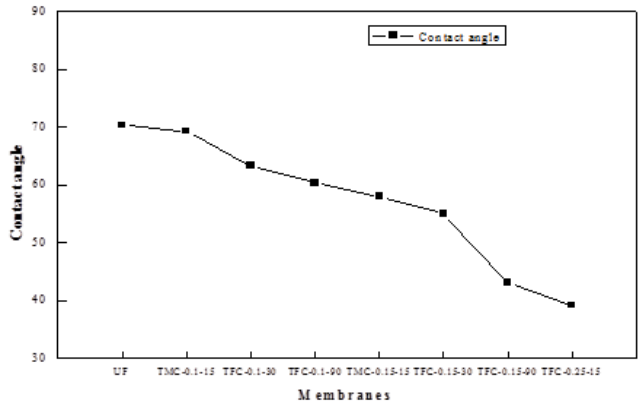

Fig. 7. Contact angle of water on the surface of membranes prepared.

4.5. PWP and porosity

The PWP and the porosity of the CA support and the thin film composite are illustrated in Fig. 8. The PWP decreased significantly from 23.57 to 10.44 L m^{-2} h^{-1} bar^{-1} when the reaction time and TMC concentration increased. The range of values accorded previously for nanofiltration membrane [2]. In dead as, the concentration of TMC increased, the layer of the thin film composite was postulated to be thicker and thus, resulted in lower permeability's (as it can be seen in SEM images (Fig. 4). Also, longer reaction time will induce a thicker skin film layer on top of the CA ultrafiltration support [21]. It can be noticed that the same trends for porosity decreased from 70.16% to 40%. This is on accordance with the fact that the water permeability is affected by porosity and membrane thickness.

4.6. Water content

The results of WC calculated using Eq. (2) for the UF support and NF-TFC membranes are presented in Fig. 9. The WC decreased from 70.80% to 45% when time reaction and TMC concentration increase. The WC seems to be affected by the decrease of porosity.

4.7. Effect of TMC concentration

The monomer concentration is an important parameter for IP that influences the performance of prepared TFC-NF membranes. Fig. 10 shows the performance of the TFC-NF membrane prepared using different TMC concentrations, keeping the other parameter constant (MPD = 0.2% (w/v), T = 25°C and time = 2 min). Initially, the water permeability declined rapidly from 23.57 to 10.44 L h^{-1} m^{-2} bar^{-1} as the TMC concentration increased Between 0% to 0.25% (w/v). Also, the rejection of Na_2SO_4 and NaCl solutions increased from 69.23% to 92.43% and from 19% to 55.54%, respectively, when the TMC concentration increased. The permeability and salts rejection behavior of the monomer concentration can be justified in terms of morphology and chemical changes of the membrane that occur during the formation of skin film. The TMC concentration has a great effect on the interfacial

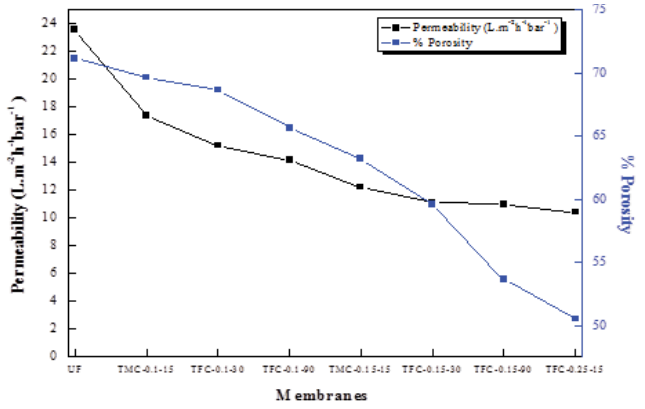

Fig. 8. Variation of pure water permeation and porosity with TMC concentration (amine = 2%; curing temperature = 25°C; curing time = 2 min).

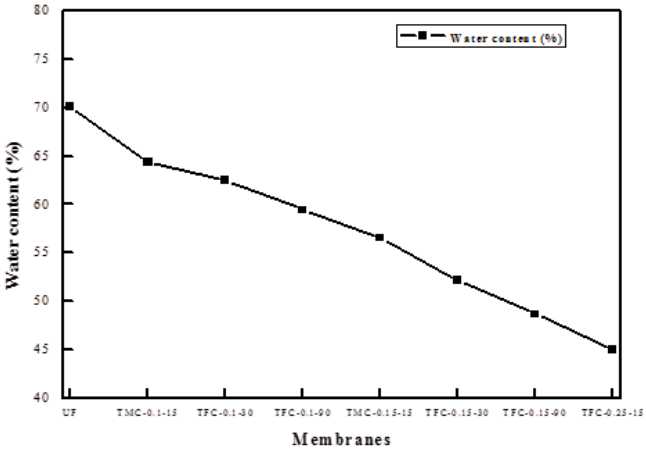

Fig. 9. Water content for UF support and NF-TMC.

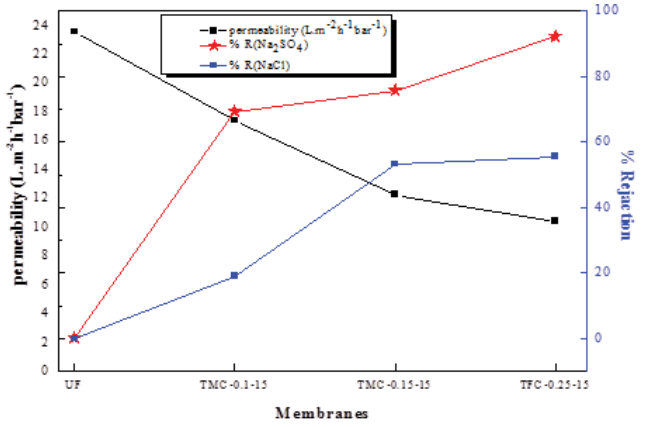

Fig. 10. Variation of membrane performance with TMC concentration ([MPD] = 0.2%; time (MPD) = 2 min, [Na_2SO_4] = [NaCl] = 1 g L^{-1}, P = 9 bar and T = 25°C).

polymerization and thereby the morphology and thickness of the prepared polyamide skin layer [22,44]. At lower TMC concentration, the rate of polymerization reaction is expected to be lower due to the non availability of sufficient monomer concentration at the interfacial polymerization site [22,44]. This results where taker formation of thin and loose polyamide thin top layer which poorly rejects the salts while permeating more amount of water. The increase of the TMC concentration leads to increase the MPD collided with TMC and the cross-linking extent of skin layer [22,45–49].

4.8. Effect of reaction time

To study the influence of reaction time on the membrane performance, a series of TFC membranes were prepared at different times. The results of PWP and salts (Na_2SO_4, NaCl) rejection are represented in Fig. 11. It can be observed from Fig. 11 that Na_2SO_4 and NaCl rejections, and also the water permeability increase on increasing the reaction time in organic phase with TMC for polyamide skin layer. The water permeability decreased from 23.57 to 11 L m^{-2} h^{-1} bar^{-1} and salts rejection increased from 75.76% to 78.98 % and from

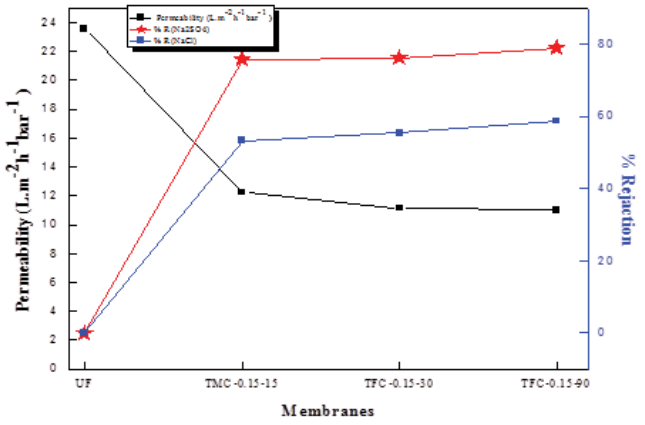

Fig. 11. Variation of NaCl rejection and water flux on interfacial reaction time of TMC ([MPD] = 0.2%; time (MPD) = 2 min, [Na_2SO_4] = [NaCl] = 1 g L^{-1}, P = 9 bar and T = 25°C).

53.3 to 58,76 for Na_2SO_4 and NaCl, respectively, when the reaction time varied from 15 to 90 s. The maximum rejection for Na_2SO_4 was reaching 78.98% at 90 s, while the water permeability was 11 L m^{-2} h^{-1} bar^{-1}. At a short reaction time (15 s), the polyamide top surface was not completely formed and it was thin on the top of CA support (as it can be seen in SEM images), which leaded to a high water permeability and low salts rejection. The increasing of reaction time leads the novel prepared skin top surface to become thicker and the cross-linking extent to become higher.

However, after predetermined reaction time, the water permeability and rejection of salts nearly stayed constant, which can be explained by the self-limiting phenomenon in IP technique [45]. The cross-linking and thicker extent was increased, and numbers of COOH groups existed on the TFC membrane, this by decreasing the salts rejection and water permeability. It was well known that IP technique was a self-limiting phenomenon offered in the diffusion-controlled IP [29,45].

4.9. Effects of operating parameters on the removal of cadmium

4.9.1. Effect of feed concentration

The effect of feed concentration on the retention efficiency of CA support and TFC-NF membranes at 25°C and at pH = 6.8 is presented in Fig. 12. As observed in this figure, an increase of the salt concentration leads to a decrease of cadmium retention. This result could be justified by the appearance of the concentration polarization phenomenon at the interface membrane-solution [50,51]. This layer, by neutralization of negative charges of the membrane [50], reduces the repulsion force between the anions present in solution and membrane surface, so by consequence the cadmium permeate easily circulates through the membrane.

4.9.2. Effect of the nature of associated anion

The results of the retention of three cadmium salts ($CdSO_4$, $CdCl_2$, $Cd(NO_3)_2$) having different associated

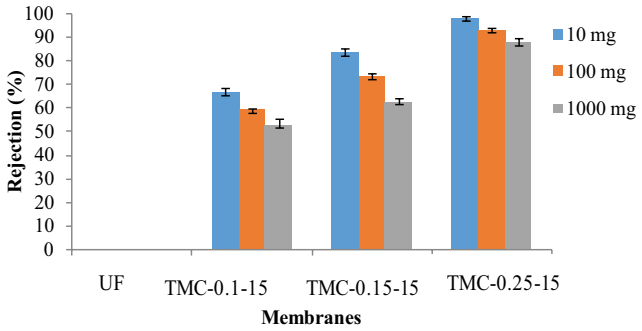

Fig. 12. Dependency of cadmium retention on the feed concentration Cd $(NO_3)_2$ salt (pH = 6.8, T = 25°C and P = 9 bar).

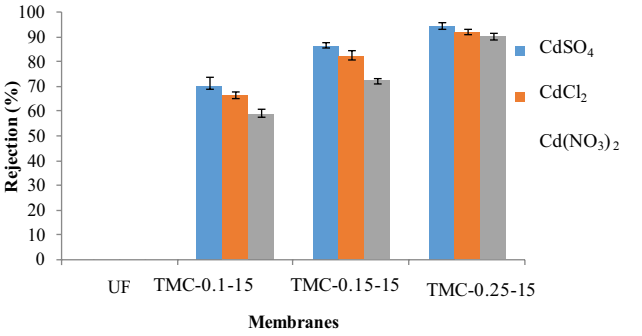

Fig. 13. Dependency of cadmium retention on the salt nature ([Cd^{2+}] = 100 mg L^{-1}, pH = 6.8, and T = 25°C, and P = 9 bar).

anions are shown in Fig. 13. The sequence of cadmium salt retention by the membranes is R($Cd(NO_3)_2$) < R($CdCl_2$) < R ($CdSO_4$). The cadmium associated with the divalent anion (SO_4^{2-}) is more rejected than the cadmium associated with monovalent anions (Cl^- and NO_3^-). The cadmium rejection depends on the anion valence, which is related to the electrostatic repulsion force exerted by the TFC-NF membranes on the more loaded anion. Comparing the retention of $CdCl_2$ and $Cd(NO_3)_2$, the retention order could be related to the hydration energy (HE) of chloride and nitrate anions, as reported in Table 3.The less hydrated ions penetrate more easily through the membrane surface, thus resulting in a lower retention of cadmium associated with nitrate anions [52].

4.9.3. Effect of pH

Generally, the pH affects the charge of the nanofiltration membrane and the anions of solutes in solution and as consequence the membrane efficiency. Here, we investigated the rejection of cadmium salts at three pH (pH = 3, pH = 5 and pH = 8). The concentration of cadmium salts and the trans-membrane pressure (TMP) were fixed at 1 g L^{-1} and 9 bar, respectively. From Fig. 14 we noted that at pH = 3, the membrane is positively charged (protoned species A-NH_3^+). The increase of the cadmium retention rate can be attributed to the repulsion between cadmium (Cd^{2+}) and the positive charge of the membrane. At pH = 5, the retention rate was

Table 3
Hydration energy of ions used in this work [8]

Ions	Hydration energy (KJ mol^{-1})
NO_3^-	310
Cl^-	325
Cd^{2+}	1,815
SO_4^{2-}	1,047

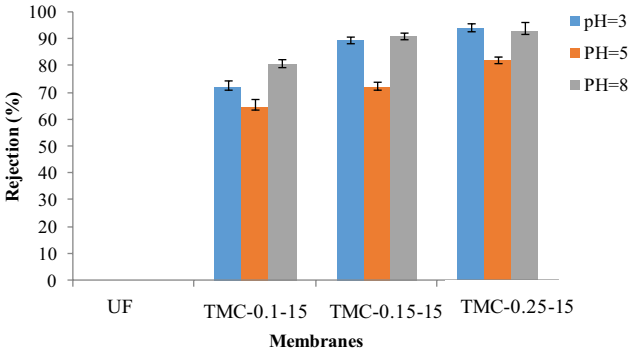

Fig. 14. Dependency of cadmium retention on pH ([Cd^{2+}] = 100 mg L^{-1}, P = 9 bar and T = 25°C).

slightly decreased. This value is an indication of isoelectric point (PEI) of membranes because it corresponds to a minimum of cadmium rejection. While at pH = 8, above the isoelectric point, the membrane is charged negatively, which corresponds to a deprotonation of the carboxylic group (R–COO^-). Our results are in concordance with the literature [48]. Furthermore, the increasing of cadmium retention below the isoelectric pH is attributed to repulsion between the nitrate anion and the negative charge of the membrane. This can be explained by the absence of the repulsive forces between the uncharged membrane surface and the ions in solution [53].

5. Conclusions

Novel flat-sheet thin film composite membranes for nanofiltration were successfully prepared through interfacial polymerization of MPD and TMC on CA ultrafiltration membrane. The membrane performance, that is, the water permeability and salts rejection of the TFC-NF are strongly dependent on the polyamide thin top layer preparation condition such as reaction time and TMC concentration. SEM and AFM images showed that the TFC had smooth surface. The water permeability decreased from 23.35 to 10.44 L m^{-2} h^{-1} bar^{-1}, when TMC concentration and reaction time increased. In addition, the salts rejections of these TFC membranes were varied from 69.23% to 92.43% and from 19% to 55.54% by using Na_2SO_4 and NaCl, respectively. The rejection of cadmium depends on the nature of associated anion: ($Cd(NO_3)_2$) < R($CdCl_2$) < R($CdSO_4$).

Symbols

J	—	Flux, L m^{-2} h^{-1}
V	—	Volume of pure water, L
A	—	Area of the membrane, m^2
Δt	—	Time, h
R	—	Rejection, %
C_f	—	Feed concentration, g L^{-1}
C_p	—	Permeate concentration, g L^{-1}
W_w	—	Weight of the membrane wet, g
W_d	—	Weight of the membrane dry, g

Acknowledgements

This work was supported by CERTE, Technopark Borj-Cedria (Tunisia) and Institute on Membrane Technology ITM, Italy.

References

[1] Y.F. Li, Y.L. Su, Y. Dong, X.T. Zhao, Z.Y. Jiang, R. Zhang, J.J. Zhao, Separation performance of thin-film composite nanofiltration membrane through interfacial polymerization using different amine monomers, Desalination, 333 (2014) 59–65.
[2] A.W. Mohammad, Y.H. Teow, W.L. Ang, Y.T. Chung, D.L. Oatley-Radcliffe, N. Hilal, Nanofiltration membranes review: recent advances and future prospects, Desalination, 356 (2015) 226–254.
[3] R. López-Roldán, A. Rubalcaba, J. Martin-Alonso, S. González, V. Martí, J.L. Cortina, Assessment of the water chemical quality improvement based on human health risk indexes: application to a drinking water treatment plant incorporating membrane technologies, Sci. Total Environ., 540 (2016) 334–343.
[4] M.H. Liu, Q. Chen, K. Lu, W.Q. Huang, Z.H. Lü, C.M. Zhou, S.C. Yu, C.J. Gao, High efficient removal of dyes from aqueous solution through nanofiltration using diethanolamine-modified polyamide thin-film composite membrane, Sep. Sci. Technol., 173 (2017) 135–143.
[5] H. Elcik, S.O. Celik, M. Cakmakci, B. Özkaya, Performance of nanofiltration and reverse osmosis membranes for arsenic removal from drinking water, Desal. Wat. Treat., 57 (2016) 20422–20429.
[6] M. Mojarrad, A. Noroozi, A. Zeinivand, P. Kazemzadeh, Response surface methodology for optimization of simultaneous Cr (VI) and as (V) removal from contaminated water by nanofiltration process, Environ. Prog. Sustainable Energy, 37 (2018) 434–443.
[7] P. Mikulášek, J. Cuhorka, Removal of heavy metal ions from aqueous solutions by nanofiltration, Chem. Eng. Trans., 47 (2016) 379–384.
[8] L.B. Chaudhari, Z.V.P. Murthy, Separation of Cd and Ni from multicomponent aqueous solutions by nanofiltration and characterization of membrane using IT model, J. Hazard. Mater., 180 (2010) 309–315.
[9] Y.H. Li, S. Wang, Z. Luan, J. Ding, C. Xu, D. Wu, Adsorption of cadmium (II) from aqueous solution by surface oxidized carbon an tubes, Carbon, 41 (2003) 1057–1062.
[10] C.W. Cheung, J.F. Porter, G. Mckay, Sorption kinetic analysis for the removal of cadmium ions from effluents using bone char, Water Res., 35 (2001) 605–612.
[11] J. Gao, S.-P. Sun, W.-P. Zhu, T.-S. Chung, Green modification of outer selective P84 nanofiltration (NF) hollow fiber membranes for cadmium removal, J. Membr. Sci., 499 (2016) 361–369.
[12] Y. Garba, S. Taha, J. Cabon, G. Dorange, Modeling of cadmium salts rejection through a nanofiltration membrane: relationships between solute concentration and transport parameters, J. Membr. Sci., 211 (2003) 51–58.
[13] X.-L. Wang, J.-F. Wei, Z. Dai, K.-Y. Zhao, H. Zhang, Preparation and characterization of negatively charged hollow fiber nanofiltration membrane by plasma-induced graft polymerization, Desalination, 286 (2012) 138–144.
[14] S. Mondal, S.R. Wickramasinghe, Photo-induced graft polymerization of *N*-isopropyl acrylamide on thin film composite membrane: Produced water treatment and antifouling properties, Sep. Sci. Technol., 90 (2012) 231–238.
[15] R.H. Lajimi, A.B. Abdallah, E. Ferjani, M.S. Roudesli, A. Deratani, Change of the performance properties of nanofiltration cellulose acetate membranes by surface adsorption of polyelectrolyte multilayers, Desalination, 163 (2004) 193–202.
[16] M.N.A. Seman, M. Khayet, Z.I.B. Ali, N. Hilal, Reduction of nanofiltration membrane fouling by UV-initiated graft polymerization technique, J. Membr. Sci., 355 (2010) 133–141.
[17] J.E. Cadotte, R.J. Petersen, R.E. Larson, E.E. Erickson, A new thin-film composite seawater reverse osmosis membrane, Desalination, 32 (1980) 25–31.
[18] X.Z. Wei, X. Kong, J. Yang, G.L. Zhang, J.Y. Chen, J.D. Wang, Structure influence of hyperbranched polyester on structure and properties of synthesized nanofiltration membranes, J. Membr. Sci., 440 (2013) 67–76.
[19] X. Wang, T.-M. Yeh, Z. Wang, R. Yang, R. Wang, H.Y. Ma, B.S. Hsiao, B. Chu, Nanofiltration membranes prepared by interfacial polymerization on thin-film nanofibrous composite scaffold, Polymer, 55 (2014) 1358–1366.
[20] A. Soroush, J. Barzin, M. Barikani, M. Fathizadeh, Interfacially polymerized polyamide thin film composite membranes: preparation, characterization and performance evaluation, Desalination, 287 (2012) 310–316.
[21] M.N.A. Seman, M. Khayet, N. Hilal, Nanofiltration thin-film composite polyester polyethersulfone-based membranes prepared by interfacial polymerization, J. Membr. Sci., 348 (2010) 109–116.
[22] J. Cheng, W.X. Shi, L.H. Zhang, R.J. Zhang, A novel polyester composite nanofiltration membrane formed by interfacial polymerization of pentaerythritol (PE) and trimesoyl chloride (TMC), Appl. Surf. Sci., 416 (2017) 152–159.
[23] L.H. Wang, D.L. Li, L.H. Cheng, L. Zhang, H.L. Chen, Synthesis of 4-aminobenzoylpiperazine for preparing the thin film composite nanofiltration membrane by interfacial polymerization with TMC, Sep. Sci. Technol., 48 (2013) 466–472.
[24] T.M. Mayhew, G.J. Burton, Stereology and its impact on our understanding of human placental functional morphology, Microsc. Res. Tech., 38 (1997) 195–205.
[25] W. Xie, G.M. Geise, B.D. Freeman, H.-S. Lee, G.S. Byun, J.E. McGrath, Polyamide interfacial composite membranes prepared from *m*-phenylene diamine, trimesoyl chloride and a new disulfonated diamine, J. Membr. Sci., 403 (2012) 152–161.
[26] M. Jenkins, M.B. Tanner, Operational experience with a new fouling resistant reverse osmosis membrane, Desalination, 119 (1998) 243–249.
[27] X.C. Fan, Y. Dong, Y.L. Su, X.T. Zhao, Y.F. Li, J.Z. Liu, Z.Y. Jiang, Improved performance of composite nanofiltration membranes by adding calcium chloride in aqueous phase during interfacial polymerization process, J. Membr. Sci., 452 (2014) 90–96.
[28] T. Tsuru, S. Sasaki, T. Kamada, T. Shintani, T. Ohara, H. Nagasawa, K. Nishida, M. Kanezashi, T. Yoshioka, Multilayered polyamide membranes by spray-assisted 2-step interfacial polymerization for increased performance of trimesoyl chloride (TMC)/*m*-phenylenediamine (MPD)-derived polyamide membranes, J. Membr. Sci., 446 (2013) 504–512.
[29] M.N.A. Seman, M. Khayet, N. Hilal, Development of antifouling properties and performance of nanofiltration membranes modified by interfacial polymerisation. Desalination, 273 (2011) 36–47.
[30] S.-Y. Kwak, M.-O. Yeom, I.J. Roh, D.Y. Kim, J.-J. Kim, Correlations of chemical structure, atomic force microscopy (AFM) morphology, and reverse osmosis (RO) characteristics in aromatic polyester high-flux RO membranes, J. Membr. Sci., 132 (1997) 183–191.
[31] X. Li, Y.M. Cao, H.J. Yu, G.D. Kang, X.M. Jie, Z.N. Liu, Q.A Yuan, A novel composite nanofiltration membrane prepared with PHGH and TMC by interfacial polymerization, J. Membr. Sci., 466 (2014) 82–91.

[32] E. Ferjani, E. Ellouze, R.B. Amar, Treatment of seafood processing wastewaters by ultrafiltration-nanofiltration cellulose acetate membranes, Desalination, 177 (2005) 43–49.
[33] A. Figoli, C. Ursino, F. Galiano, E. Di Nicolò, P. Campanelli, M.C. Carnevale, A. Criscuoli, Innovative hydrophobic coating of perfluoropolyether (PFPE) on commercial hydrophilic membranes for DCMD application, J. Membr. Sci., 522 (2017) 192–201.
[34] C. Ursino, S. Simone, L. Donato, S. Santoro, M.P. De Santo, E. Drioli, E. Di Nicolò, A. Figoli, ECTFE membranes produced by non-toxic diluents for organic solvent filtration separation, RSC Adv., 6 (2016) 81001–81012.
[35] A.K. Ghosh, E.M.V. Hoek, Impacts of support membrane structure and chemistry on polyamide–polysulfone interfacial composite membranes, J. Membr. Sci., 336 (2009) 140–148.
[36] Y.J. Zeng, L.H. Wang, L. Zhang, J.Q. Yu, An acid resistant nanofiltration membrane prepared from a precursor of poly(s-triazine-amine) by interfacial polymerization, J. Membr. Sci., 546 (2018) 225–233.
[37] G.N.B. Baroña, J. Lim, M.J. Choi, B. Jung, Interfacial polymerization of polyamide-aluminosilicate SWNT nanocomposite membranes for reverse osmosis, Desalination, 325 (2013) 138–147.
[38] B. Tang, Z.B. Huo, P.Y. Wu, Study on a novel polyester composite nanofiltration membrane by interfacial polymerization of triethanolamine (TEOA) and trimesoyl chloride (TMC): I. Preparation, characterization and nanofiltration properties test of membrane, J. Membr. Sci., 320 (2008) 198–205.
[39] M. Jahanshahi, A. Rahimpour, M. Peyravi, Developing thin film composite poly(piperazine-amide) and poly(vinyl-alcohol) nanofiltration membranes, Desalination, 257 (2010) 129–136.
[40] L.M. Jin, S.L. Yu, W.X. Shi, X.S. Yi, N. Sun, Y.L. Ge, C. Ma, Synthesis of a novel composite nanofiltration membrane incorporated SiO_2 nanoparticles for oily wastewater desalination, Polymer, 53 (2012) 5295–5303.
[41] L.Y. Ng, A.W. Mohammad, C.P. Leo, N. Hilal, Polymeric membranes incorporated with metal/metal oxide nanoparticles: a comprehensive review, Desalination, 308 (2013) 15–33.
[42] S.S. Bing, J.Q. Wang, H. Xu, Y.Y. Zhao, Y. Zhou, L. Zhang, C.J. Gao, L.A. Hou, Polyamide thin-film composite membrane modified with persulfate for improvement of perm-selectivity and chlorine-resistance, J. Membr. Sci., 555 (2018) 318–326.
[43] C.Y. Tang, Y.-N. Kwon, J.O. Leckie, Effect of membrane chemistry and coating layer on physiochemical properties of thin film composite polyamide RO and NF membranes: I. FTIR and XPS characterization of polyamide and coating layer chemistry, Desalination, 242 (2009) 149–167.
[44] L. Li, S.B. Zhang, X.S. Zhang, Preparation and characterization of poly(piperazineamide) composite nanofiltration membrane by interfacial polymerization of 3,3′,5,5′-biphenyl tetraacyl chloride and piperazine, J. Membr. Sci.. 33 (2009) 133–139.
[45] P.R. Buch, D.J. Mohan, A.V.R. Reddy, Preparation, characterization and chlorine stability of aromatic–cycloaliphatic polyamide thin film composite membranes, J. Membr. Sci., 309 (2008) 36–44.
[46] B.B. Tang, C. Zou, P.Y. Wu, Study on a novel polyester composite nanofiltration membrane by interfacial polymerization. II. The role of lithium bromide in the performance and formation of composite membrane, J. Membr. Sci., 365 (2010) 276–285.
[47] Y.J. Song, P. Sun, L.L. Henry, B.H. Sun, Mechanisms of structure and performance controlled thin film composite membrane formation via interfacial polymerization process, J. Membr. Sci., 251 (2005) 67–79.
[48] A.W. Mohammad, N. Hilal, M.N. Abu Seman, A study on producing composite nanofiltration membranes with optimized properties, Desalination, 158 (2003) 73–78.
[49] J. Ji, M. Mehta, Mathematical model for the formation of thin-film composite hollow fiber and tubular membranes by interfacial polymerization, J. Membr. Sci., 192 (2001) 41–54.
[50] J. Kheriji, D. Tabassi, B. Hamrouni, Removal of Cd(II) ions from aqueous solution and industrial effluent using reverse osmosis and nanofiltration membranes, Water Sci. Technol., 72 (2015) 1206–1216.
[51] G.T. Ballet, L. Gzara, A. Hafiane, M. Dhahbi, Transport coefficients and cadmium salt rejection in nanofiltration membrane, Desalination, 167 (2004) 369–376.
[52] R. Epsztein, E. Shaulsky, N. Dizge, D.M. Warsinger, M. Elimelech, Ionic charge density-dependent Donnan exclusion in nanofiltration of monovalent anions, Environ. Sci. Technol., (2018) doi: 10.1021/acs.est.7b06400.
[53] B.A.M. Al-Rashdi, D.J. Johnson, N. Hilal, Removal of heavy metal ions by nanofiltration, Desalination, 315 (2013) 2–17.